

This item is the archived peer-reviewed author-version of:

Enhancing bioflocculation in high-rate activated sludge improves effluent quality yet increases sensitivity to surface overflow rate

Reference:

Van Winckel Tim, Ngo Nam, Sturm Belinda, Al-Omari Ahmed, Wett Bernhard, Bott Charles, Vlaeminck Siegfried, De Clippeleir Haydée.- Enhancing bioflocculation in high-rate activated sludge improves effluent quality yet increases sensitivity to surface overflow rate
Chemosphere - ISSN 1879-1298 - 308:2(2022), 136294

Full text (Publisher's DOI): <https://doi.org/10.1016/J.CHEMOSPHERE.2022.136294>
To cite this reference: <https://hdl.handle.net/10067/1901870151162165141>

1 **Enhancing bioflocculation in high-rate activated sludge increases sensitivity to changes in**
2 **surface overflow rate while improving effluent quality**

3 *Tim Van Winckel^{1,2,3}, Nam Ngo^{2,4}, Belinda Sturm³, Ahmed Al-Omari², Bernhard Wett⁵, Charles*
4 *Bott⁶, Siegfried E. Vlaeminck^{7*}, Haydée De Clippeleir²*

5

6 *¹Center of Microbial Ecology and Technology (CMET), Faculty of Bioscience Engineering, Ghent*
7 *University, 9000 Gent, Belgium*

8 *²District of Columbia Water and Sewer Authority, Blue Plains Advanced Wastewater Treatment Plant,*
9 *5000 Overlook Ave, SW Washington, DC 20032, USA*

10 *³Department of Civil, Environmental and Architectural engineering, The University of Kansas, KS, USA*

11 *⁴Department of Civil and Environmental Engineering, The Catholic University of America, Washington*
12 *DC, USA*

13 *⁵ARA consult GmbH, Innsbruck, Austria*

14 *⁶Hampton Roads Sanitation District, VA, USA*

15 *⁷Research Group of Sustainable Energy, Air and Water Technology, Department of Bioscience*
16 *Engineering, University of Antwerp, 2020 Antwerpen, Belgium*

17

18 **Corresponding author: siegfried.vlaeminck@uantwerpen.be*

19

20 **Abstract**

21 High-rate activated sludge (HRAS) depends on good bioflocculation and subsequent solid-liquid
22 separation to maximize the capture of organics. However, full-scale applications often suffer from
23 poor and unpredictable effluent suspended solids (ESS). While the biological aspects of
24 bioflocculation are thoroughly investigated, the effects of fines (settling velocity $< 0.6 \text{ m}^3/\text{m}^2/\text{h}$),
25 shear and surface overflow rate (SOR) are unclear. This work tackled the impact of fines, shear,
26 and SOR on the ESS in absence of settleable influent solids. This was assessed on a full-scale
27 HRAS step-feed (SF) and pilot-scale contact-stabilization (CS) configuration using batch settling
28 tests, controlled clarifier experiments, and continuous operation of reactors. Fines contributed to
29 25% of the ESS in the full-scale SF configuration. ESS decreased up to 30 mg TSS/L when
30 bioflocculation was enhanced with the CS configuration. The feast-famine regime applied in CS
31 promoted the production of high-quality extracellular polymeric substances (EPS). However, this
32 resulted in a narrow and unfavorable settling velocity distribution, with $50\% \pm 5\%$ of the sludge
33 mass settling between $0.6\text{-}1.5 \text{ m}^3/\text{m}^2/\text{h}$, thus increasing sensitivity towards SOR changes. A low
34 shear environment (20 s^{-1}) before the clarifier for at least one minute was enough to ensure the
35 best possible settling velocity distribution, regardless of prior shear conditions. Overall, this paper
36 provides a more complete view on the drivers of ESS in HRAS systems, creating the foundation
37 for the design of effective HRAS clarifiers. Tangible recommendations are given on how to
38 manage fines and establish the optimal settling velocity of the sludge.

39

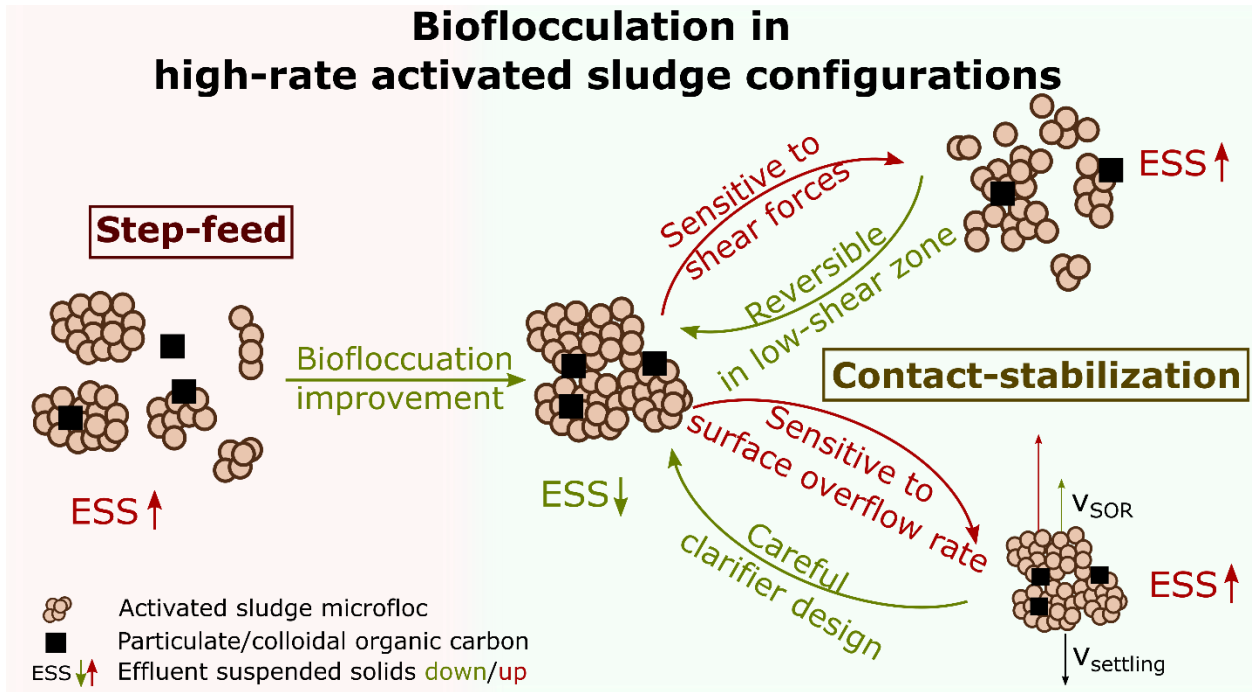
40 **Keywords:** A-stage, floc formation, sewage, settling, wastewater

41 List of Acronyms

AWTP	Advanced wastewater treatment plant
BSA	bovine serum albumin
CEPT	Chemically enhanced primary treatment
COD	Chemical oxygen demand
CS	Contact-stabilization
CSV	Critical settling velocity
DO	Dissolved oxygen
EPS	Extracellular polymeric substances
ESS	Effluent suspended solids
F/M	Food-to-microorganism
HRAS	High-rate activated sludge
ISV	Initial settling velocity
LB	Loosely-bound
OHO	Ordinary heterotrophs
PN	Protein
PS	Polysaccharides
SF	Step-feed
SLR	Sludge loading rate
SOR	Surface overflow rate
SRT	Solids retention time
SVI	Sludge volume index
TB	Tightly-bound
TOF	Threshold of flocculation
TSS	Total suspended solids
vOUR	Volumetric loading rate

42

43



45

46

47 **1. Introduction**

48 High-rate activated sludge (HRAS) is a promising technology to maximize the diversion of
49 carbon through from the water to the solids line. The technology works on the principle that
50 carbon present in the wastewater is converted to a harvestable form (carbon redirection) by
51 converting incoming COD into particulate biomass in combination with adsorption of particulate
52 and colloidal COD onto the biomass and storage of soluble COD in the cell. Both adsorption and
53 storage, frequently lumped together as ‘biosorption’, are carbon removal processes with do not
54 require oxidation and thus further increase the observed yield of the biomass (Guellil et al., 2001;
55 Rahman et al., 2017; Ullrich and Smith, 1951). This particulate form of COD, made up out of
56 biomass and adsorbed/stored influent organics, can be subsequently captured in the clarifier and
57 send to the solids processing line (carbon capture) for biogas production or upgraded commodities
58 (Alloul et al., 2018). Carbon redirection in HRAS is commonly achieved by operating an
59 extremely short solids retention time (SRT) of 0.2 - 0.8 days and high organic loading rate (> 2 g
60 COD/L/d) depending on the reactor configuration. This short sludge age reduces the amount of
61 oxidation of carbonaceous organics to CO_2 and limits the endogenous respiration of the sludge
62 contributing contribution to CO_2 formation (Cagnetta et al., 2019; De Graaff & Roest, 2012;
63 Jimenez et al., 2015; Meerburg et al., 2015; Rahman et al., 2016). However, shortening the SRT
64 leads to diminishing returns in terms of carbon capture due to increased stress on the
65 bioflocculation mechanism, creating bioflocculation limitations (Rahman et al., 2016).

66 In this study, bioflocculation is defined as the ability of the sludge to form (macroscopic) flocs in
67 the clarifier with a settling velocity greater than the upflow velocity imposed by the surface
68 overflow rate (SOR) in the clarifier. Bioflocculation is thus a driver for the settling behavior of
69 the sludge within the clarifier and is therefore directly correlated with the observed effluent
70 suspended solids (ESS) (Murthy, 1998; Urbain et al., 1993). A bioflocculation limitation is
71 subsequently defined as the manifestation of an increase in ESS because of inadequate floc
72 formation. HRAS systems report out ESS numbers in range of 30 – 83 mg total suspended solids
73 per liter (TSS/L) (Cagnetta et al., 2019; De Graaff and Roest, 2012; Rahman et al., 2019), while
74 conventional, long SRT systems typically achieve 8-19 mg TSS/L (EPA, 2013). Additionally,
75 SRT is not a good predictor of effluent suspended solids in practice. The full-scale A-stage
76 reactors operated in the Netherlands all operate around the same aerobic SRT (~ 0.2 days), yet all

77 report out different ESS (De Graaff and Roest, 2012). The reason for this poor correlation is
78 unknown, but given that factors such as influent composition, reactor and clarifier design, shear
79 forces, and more influences the final ESS, the effect of SRT was probably not strong enough to
80 dictate this correlation.

81 Bioflocculation is mediated by extracellular polymeric substances (EPS) produced by the biomass
82 in the reactor (Sheng et al., 2010). For HRAS systems, the influent strength and characteristics
83 are the main driver for EPS production. For medium to high-strength raw wastewater, EPS
84 production is predominantly driven by the food-to-microorganism (F/M) rate (Rahman et al.,
85 2017; Sturm et al., 2016). For low-strength wastewaters or chemically enhanced primary
86 treatment (CEPT) effluent, a proper feast-famine regime seems to be important to drive the
87 production of EPS as applied in the contact-stabilization (CS) configuration (Rahman et al.,
88 2019). Contact-stabilization, first described by Coombs (1922), utilizes return activated sludge
89 aeration (i.e. “stabilization) in the stabilizer zone, before bringing into contact with the sewage in
90 contactor under a short hydraulic retention time. This configuration utilizes feast (contactor) and
91 famine (stabilizer) conditions in the process, inducing EPS production (Rahman et al., 2019). An
92 important aspect of bioflocculation is the capture of ‘fines’, i.e. particulate solids that settle slower
93 than $0.6 \text{ m}^3/\text{m}^2/\text{h}$ (within flocculation time of 10 min). Fines get enmeshed into the flocs with the
94 help of free binding spots on the EPS, thus improving effluent quality (Van Winckel et al., 2019).
95 However, the effect of increased fines load on the ESS in continuous systems with or without
96 proper bioflocculation is poorly understood.

97 While the positive impact of improved bioflocculation on process performance is known (Jimenez
98 et al., 2015; Rahman et al., 2016), its influence on the settling velocity distribution is unknown.
99 Additionally, the effect of shear and fines loading within the context of bioflocculation on the
100 distribution is not well understood. Hydraulic variations in or prior to the clarifier, like changes
101 in SOR or shear forces, can have a detrimental effect on effluent quality regardless of how well
102 bioflocculation is maintained. HRAS systems operate at a higher SOR ($0.75 - 1.4 \text{ m}^3/\text{m}^2/\text{h}$) (De
103 Graaff & Roest, 2012) than most conventional clarifiers ($0.6 - 1 \text{ m}^3/\text{m}^2/\text{h}$) (WEF, 2005). Because
104 the typical settling velocity distribution of HRAS sludge is unknown, the effect of elevated SOR
105 on effluent suspended solids remains unclear. HRAS could have a higher sensitivity towards SOR
106 changes in a HRAS clarifier. Sensitivity here is defined as degree of change in effluent suspended

107 solids induced by a change in SOR in the HRAS clarifier. A low sensitivity to SOR changes is
108 preferred because this widens the operational range of the clarifier where no significant increase
109 in ESS is observed. However, a severe bioflocculation limitation may lead to a low sensitivity,
110 but a high effluent suspended number across the operational range of the HRAS clarifier. To this
111 date, there is no clear recommendation on optimal SOR ranges a HRAS clarifier should operate
112 in. Additionally, high shear before the clarifier can disrupt flocs and alter the settling velocity
113 distribution, thus changing how the SOR will impact effluent quality.

114 Traditionally, clarifier performance in activated sludge systems is assessed using ‘classical’
115 clarifier metrics, such as sludge volume index (SVI) which measures volume of the settled sludge
116 bed after a predetermined amount of time (typically 30 minutes) and initial settling velocity (ISV)
117 which is the maximum settling speed of the sludge bed. However, these metrics have been shown
118 to be unreliable as they overemphasize the importance of hindered settling and compression in a
119 clarifier which correlates poorly with effluent quality, especially in HRAS systems (Mancell-
120 Egala et al., 2017; Mancell-Egala et al., 2016). Moreover, Granular systems also report out great
121 SVIs but often fail to adequately capture fines (Li et al., 2008; Rocktäschel et al., 2015). Most
122 HRAS systems are fed with raw wastewater which potentially obscures the link between physical
123 parameters (SOR, shear,...) and bioflocculation, driven by biological parameters. Rinas et al.
124 (2018) determined that, on average, 15% of solids travel faster than $1.2 \text{ m}^3/\text{m}^2/\text{h}$ during dry
125 weather condition. This can increase up to 40% during wet weather. These solids can potentially
126 provide ballast for flocs and improve suspended solids removal without the need for flocculation.
127 This also turns the HRAS system into a form of primary clarifier at very short SRT, further
128 obscuring the link between effluent suspended solids with EPS production. Kinyua et al. (2017)
129 found a low correlation between EPS and bioflocculation for a HRAS pilot treating raw
130 wastewater. The four A-stage installations in the Netherlands all report very low SVI numbers
131 (60 – 80 mL/g TSS), despite dealing with limitations in the clarifiers (De Graaff & Roest, 2012).
132 No rigorous experimental work has been performed thus far on the effect of shear-induced
133 stressors on biology itself in HRAS systems.

134 This paper provides a unique perspective of two HRAS configurations operated in the absence of
135 influent solids settling faster than $0.6 \text{ m}^3/\text{m}^2/\text{h}$ (due to the presence of CEPT). This allowed for a
136 rigorous assessment of the impact of process configuration (step-feed vs contact-stabilization),

137 SOR and shear on bioflocculation and resulting effluent quality in absence of other settling drivers
138 than the biology itself. Most HRAS studies work with raw sewage and thus cannot differentiate
139 between bioflocculation-driven settling (floc formation) and other form of sedimentation (e.g fast
140 settling influent solids and inorganics). This was achieved using batch settling tests, controlled
141 clarifier experiments, and continuous reactor operation, which allowed for a clear view on the
142 settling velocity distribution of HRAS sludge and impacting factors. This work therefore creates
143 a new foundation for the design of smart and effective HRAS clarifiers, aiming at tangible
144 recommendations on how to manage fines and establish the optimal settling velocity of the sludge.
145

146 2. Material and Methods

147 2.1. Operation of the reactors

148 In this study, two configurations of the HRAS process have been utilized and investigated: A
149 pilot-scale high-rate contact-stabilization (CS) configuration and full-scale (high-rate) step-feed
150 (SF) configuration, which acts as the secondary treatment step in the Blue Plain advanced
151 wastewater treatment plant (AWTP) sewage treatment train in Washington, DC, USA.

152 The step-feed (SF) reactor used in this study was the East train of the full-scale secondary
153 treatment step at Blue Plains AWTP in Washington, DC, treating about half of the on average 1.4
154 million cubic meters of effluent from CEPT per day. The East reactor train consisted of four
155 individual parallel reactors each consisting out of four passes. The total volume of the reactor was
156 61504 m³ (~ 16.25 million gallons). RAS was introduced in pass 1, while CEPT effluent was
157 provided in pass 1, 2, and 3 depending on the incoming flow, and can thus be defined as a step-
158 feed configuration. The step-feed reactor had 14 clarifiers in operation. The clarifiers were
159 rectangular, 3.6 meters (~ 11.8 feet) deep and had a surface area of 1846 m² (~ 19870 ft²) each.
160 The SF reactor was bioaugmented with biological nutrient removal waste activated sludge (SRT
161 ~ 20 days) from the downstream reactor (Bailey Jr et al., 2008). An annotated satellite image of
162 the East reactor train can be consulted in Supplementary **Figure S1**.

163 A high-rate activated sludge pilot (volume (V) = 1000 liters), configured in a contact-stabilization
164 configuration, was operated at Blue Plains AWTP. Fresh effluent from the full-scale CEPT
165 process was continuously fed to contactor zone (V = 223 liters), where it came into contact with
166 starved sludge from the stabilizer zone (V = 223 liters). After a hydraulic retention time of 36
167 minutes, the sludge was introduced into three parallel clarifiers (Ø = 30.5 cm, V = 302 liters each).
168 The settled sludge flowed to the return activated sludge tank (V = 50 liters), which acted as a flow
169 equalizer for the pilot. The sludge was then pumped into the stabilizer zone (V = 223 liter) where
170 ample DO (> 2 mg O₂/L) was provided to oxidize sorbed organics in absence of feed. After a
171 hydraulic retention time of 88 minutes, the stabilized sludge was reintroduced in the contactor.
172 Mixing and aeration was achieved with coarse bubble aeration. Sludge wasting was achieved
173 from the contactor. A schematic of the pilot can be consulted in the Supplementary **Figure S2**.
174 Composite samples (24-hour) were automatically taken on an hourly basis from the influent,
175 effluent and WAS for further analysis. Grab samples were used for the EPS protocol.

176 *2.1.1. Contact-stabilization pilot scenarios*

177 Three scenarios were operated in the high-rate CS reactor (**Table 1**). Scenario A was
178 characterized by an aerobic contactor ($\text{DO} > 0.5 \text{ mg O}_2/\text{L}$). This was achieved by providing a
179 higher rate of coarse bubble aeration where seven seconds of continuous aeration was provided
180 per four minutes instead of one second (**Table 2**). Scenario B and C used an anoxic contactor (DO
181 $< 0.5 \text{ mg O}_2/\text{L}$) with a lower shear as a result. Scenario C has a significantly higher sludge waste
182 rate, resulting in a lower SOR compared to scenario A and B given that sludge wasting was
183 performed from the mixed liquor.

184 **2.2. Batch settling tests**

185 Batch settling test were performed to test the impact of shear and the resulting settling velocity
186 distribution (as assessed with different critical settling velocities) on the TSS capture of sludge.
187 Fresh sludge was sourced from the full-scale SF reactor and diluted to $\sim 350 \text{ mg TSS/L}$ with final
188 effluent from the full-scale plant to preserve the ionic balance. The diluted sludge was poured
189 into a modified Nalgene[®] 4L graduated cylinder ($\phi = 10 \text{ cm}$) and mechanically mixed at a fixed
190 or alternating shear rate for 10 minutes with an IKA Eurostar 60 (IKA, USA) mixer equipped
191 with two 4-bladed axial flow impellers, which are suitable for flocculation over a wide range of
192 RPMs in HRAS applications (Balemans et al., 2020). Ten minutes was chosen because this was
193 sufficient for the rate of floc formation and breakup to meet steady state conditions in previous
194 studies (Biggs & Lant, 2000; Mancell-Egala et al., 2017; Wahlberg et al., 1994). After 10 minutes,
195 the sludge was baffled with Plexiglas stick to quickly dissipate the kinetic energy and flocs were
196 allowed to settle for a predetermined amount of time. After the designated settling time, clamps
197 located five centimeters below the liquid level were opened, and sludge was allowed to rapidly
198 drain into a sample cup within about five seconds or less. The TSS collected represented the
199 fraction of total TSS that settled slower than target CSV.

200 The two degrees of freedom tested with the methodology described above were (1) shear rate and
201 (2) the critical settling velocity (CSV) of the sludge. Shear rate was mediated through mixing
202 speed, whereas CSV was varied with the settling time.

203 The investigated shear rates were 20, 55, 90, and 180 s^{-1} , which corresponded to 100, 185, 260
204 and 410 revolutions per minute (RPM) respectively. These shear rates were fixed for ten minutes

205 as described above. The effect of alternating shear was also tested. Here, the shear rate was
206 automatically and instantaneously switched between 20 and 90 s⁻¹ every one or five minutes for
207 a total of ten minutes.

208 To obtain a settling velocity distribution of the sludge at different shear rates, a range of critical
209 settling velocities were investigated. A CSV of 9, 3, 1.5, 0.6, 0.3, and 0.15 m³/m²/h was chosen
210 which corresponded to 0.33, 1, 2, 5, 10, and 20 minutes before releasing the sampling clamps.

211 **2.3. Clarifier experiments**

212 A pilot-scale clarifier (V = 99 liter, ø = 20 cm, height = 305 cm) constructed out of transparent
213 acrylic was operated in a continuous manner to determine the effects of SOR and shear in a
214 controlled environment which was representative of a full-scale clarifier. Fresh sludge was hauled
215 from the CS or SF reactor, diluted with plant process water and put in a stirred vessel which acted
216 a flow equalization tank. The sludge was then gravitationally introduced in a 20L bucket, where
217 shear was applied for 10 minutes under controlled conditions with an IKA Eurostar 60 (IKA,
218 USA) mixer equipped with two 4-bladed axial flow impellers. Next, the sludge was introduced
219 into the clarifier with Masterflex® peristaltic pumps at the midpoint of the column (152 cm). The
220 overflow and underflow of the clarifier were reintroduced in the stirred flow equalization tank.
221 The sludge's temperature was kept between 15 – 20 °C, as this was the normal operational
222 temperature of the pilot. Samples were periodically taken (at least in triplicate) after at least three
223 HRT to ensure steady state conditions.

224 The SOR (0.6 and 1.5 m³/m²/h) was changed by changing the recirculation speed over the
225 clarifier. Given the closed-loop nature of this experiment, the liquid volume (and thus liquid
226 height) in the shear bucket had to be varied to ensure a 10-minute retention time given a specific
227 SOR. As the liquid height changes the relation between RPM and the resulting shear, the RPM
228 was changed in relation with the change liquid height to ensure equal average shear throughout
229 the experiment.

230

231 **2.4. Analytical methods**

232 *2.4.1. Measurement of the particle size distribution*

233 Flocc sizes were determined by taking photographs of the formed flocs in the acrylic pilot-scale
234 clarifier. The digital camera (Canon T3i) was equipped with a 60mm f/2.8 USM macro lens and
235 focused about 1 cm deep in the clarifier. Sizes were calibrated with an adhesive ruler which was
236 put on the clarifier. Photos were taken at full resolution (18 megapixels) and analyzed with Image-
237 J 1.52n. First, contrast was enhanced by spreading the histogram so that 1% of the pixels were
238 saturated. Next, a Boolean image was created using the threshold tool where the grayscale
239 intensity was chosen at 10% of distribution. Last, the Feret diameter was determined on the
240 isolated particles, ignoring those smaller than 0.01 mm^2 , as they would be most likely noise. At
241 least 10 pictures were analyzed per sludge sample, or until the particle size distribution did not
242 change anymore.

243 *2.4.2. Other methods*

244 Total suspended solids and total Kjeldal nitrogen were measured following the standard methods
245 (APHA, 2005). COD, ammonium and phosphorus was determined using Hach® (Loveland,
246 Colorado, USA) kits following the manufacturer's instructions. COD was fractionated into total
247 COD (no pretreatment), filtered COD (sample filtered through Wattman 1.5 micrometer filter),
248 and filter-flocculated COD (flocculation-filtration with ZnSO_4 according to Mamais et al.
249 (1993)). Extracellular polymeric substances (EPS) were determined using a heat extraction
250 following the procedure described in Van Winckel et al. (2019). Protein content of the EPS was
251 determined using the modified Lowry protein assay kit (Thermo Fisher, USA) (Lowry et al.,
252 1951) with bovine serum albumin (BSA) as the standard. Polysaccharide level was determined
253 using the DuBois method with glucose as the standard (DuBois et al., 1956). Volumetric oxygen
254 uptake rate (vOUR) was determined by taking a fresh sludge sample, aerating it briefly to 5 mg
255 O_2/L DO, and measuring the declining slope in the absence of atmospheric oxygen up to a DO of
256 1 mg O_2/L . The resulting OUR was normalized to 20 °C with the standard Arrhenius coefficient
257 (1.04) (Metcalf & Eddy, 2003)

258 **2.5. Calculations**

259 Average the average velocity gradient (G, s^{-1}) was calculated using equation 1 as postulated by
260 Camp and Stein (1943):

$$G = \sqrt{\left(\frac{\epsilon}{\nu}\right)} \quad (1)$$

261 Where ϵ (m^2/s^3) is the average energy dissipation rate and ν (m^2/s) the kinematic viscosity (of
262 water). The average energy dissipation rate from an impeller could further be calculated with
263 Equation 2 by Godfrey et al. (1989):

$$\epsilon = \frac{P_o N^3 D^5}{V} \quad (2)$$

264 Where P_o (-) is the impeller's power number, which was calculated empirically based on the work
265 of Furukawa et al. (2012), N the impeller's rounds per minute (RPM), D the impeller's diameter
266 (m) and V (m^3) the volume of the container.

267 2.6. Statistical analysis

268 Two-way Student t-tests with unequal variances were performed in Microsoft excel to establish
269 statistical significance. When the p-value was smaller than 0.05, the two (normally distributed)
270 variables were considered significantly different from each other.

271

272 3. Results

273 3.1. Continuous reactor operation

274 The high-rate contact-stabilization (CS) pilot reactor was operated on CEPT effluent for three
275 distinct scenarios A, B, and C lasting 25, 31, and 22 days (28, 31, and 44 times the SRT)
276 respectively. The key differences between the scenarios were (1) measurable DO in the contactor
277 in scenario A, leading to (2) an increased shear regime in the same scenario due to more frequent
278 coarse bubble aeration, and (3) the difference in SOR (0.9 and 0.6 m³/m²/h for scenario B and C
279 respectively) due to wasting from the mixed liquor rather than the return activated sludge (**Table**
280 **2**). DO in the contactor could be ruled out based on previous work by Rahman et al. (2017), who
281 determined that a 0.5 mg O₂/L was required to induce an EPS response in this configuration.
282 Lower DO should have negatively impacted effluent quality based on the hypothesis that absence
283 of DO leads to a decrease in EPS production, discouraging bioflocculation. However, the effluent
284 suspended solids in scenario A were on average better than scenario B and C (**Table 1**),
285 discrediting the potential impact of an aerated contactor on bioflocculation.

286 Influent characteristics were typical for CEPT effluent and did not significantly differ between
287 scenarios (**Table 1**). Particulate COD was low compared to typical A-stage HRAS systems which
288 range from 200 – 400 mg particulate COD/L (De Graaff & Roest, 2012; Jimenez et al., 2015).
289 Colloidal COD was comparable to the A-stages in the Netherlands (De Graaff & Roest, 2012).
290 CEPT potentially lowered the seeding rate of active ordinary heterotrophic organisms from the
291 influent into the reactor compared to an A-stage fed with raw wastewater (Rahman et al., 2016),
292 although no measurements were performed to confirm this. The three scenarios achieved similar
293 effluent qualities in terms of soluble and colloidal COD. Effluent suspended solids (**Figure 1-IV**)
294 and particulate COD (**Table 1**) were significantly different lower in scenario C than A ($p = 0.002$
295 and 0.013 respectively), with scenario B falling in between the two. This resulted in significant
296 differences in C/N/P capture because no capture was achieved in scenario A (**Figure 1-**
297 **VI/VII/VIII**). Scenario B was able to capture 18% ± 12% of the incoming COD, the highest COD
298 capture (36% ± 16%) was achieved in scenario C. (**Figure 1-IV**).

299 Biomass activity, measured with volumetric OUR, was similar for all tested scenarios once
300 corrected for temperature. Scenario C had a low mixed liquor concentration compared to Scenario
301 B but fell within the uncertainty of scenario A (**Figure 1-III**). This resulted in a comparatively

302 shorter SRT for scenario C (**Table 2**), leading to a slightly higher redirection percentage (**Figure**
303 **1-V**). However, all three scenarios had comparable amounts of extracellular polymeric substances
304 (EPS) measured with similar quality as given by the protein over polysaccharide ratio (PN/PS)
305 (**Table 2**). EPS amount and quality has been shown to be linked with the sludge's potential to
306 bioflocculate (Sheng et al., 2010). Therefore, the operational differences observed had no impact
307 on the bioflocculation potential. Given that all biological parameters impacting bioflocculation
308 were similar between the scenarios and DO has been ruled out, the difference in effluent quality
309 was potentially explained by SOR, shear or a combination of the two.

310 **3.2. Impact of different shear regimes on TSS capture**

311 A feast-famine regime, as provided by the CS configuration, has been shown to be a major driver
312 for bioflocculation (Rahman et al., 2017). A step-feed configuration, which operates with smaller
313 substrate gradients and lacks proper feast-famine, should therefore have less favorable
314 bioflocculation potential. To test this, the impact of different shear regimes was tested on a full-
315 scale step-feed (SF) HRAS system treating the same CEPT effluent as the CS pilot. These tests
316 were performed with diluted sludge (350 mg TSS/L) to limit the number of collisions, magnifying
317 any bioflocculation limitations present. Percentage of TSS captured was used instead of absolute
318 ESS numbers as the latter do not reflect true clarifier conditions in continuous systems. Batch
319 tests do provide valuable insights in relative floc formation dynamics in a controlled environment.
320 TSS capture decreased with increasing velocity gradient regardless of the shear regime applied
321 (**Figure 2**). **Figure 2-I** shows the impact of continuous shear for 10 min ranging from 20 s^{-1} to
322 180 s^{-1} . When a velocity gradient of 90 s^{-1} was applied, the final TSS capture significantly
323 decreased at a critical settling velocity (CSV) of $0.6 \text{ m}^3/\text{m}^2/\text{h}$ and below. This indicated that a
324 continuous high shear regime had a disruptive effect on the entrapment of fines (fraction of TSS
325 $< 0.6 \text{ m}^3/\text{m}^2/\text{h}$) within the floc. At $1.5 \text{ m}^3/\text{m}^2/\text{h}$, the SOR typically associated with floc formation
326 (Mancell-Egala et al., 2017), all velocity gradients above 20 s^{-1} resulted in the same TSS capture,
327 indicating that low shear was required for the creation of flocs that settle well. At a CSV of 3
328 $\text{m}^3/\text{m}^2/\text{h}$, TSS capture was exclusively driven by settling velocity as all datapoints converged
329 (**Figure 2-I**). For this reason, $3 \text{ m}^3/\text{m}^2/\text{h}$ was not tested in **Figure 2-II/III**.

330 The shear regime in the pipes or channels leading to the clarifier is rarely constant. Mixing in the
331 channel prior to the clarifier in combination with bends, turns and other sources of head loss in

332 the piping lead to changing and often unpredictable shear forces. To account for this, the effect
333 of alternating velocity gradients, 20 and 90 s⁻¹ reflected in **Figure 2-II/III** as black and blue
334 respectively, was investigated. One minute at 20 s⁻¹ was enough to restore the floc formation to
335 similar levels achieved at 20 s⁻¹ with continuous shear in **Figure 2-I** (19% ± 4% and 22% ± 4%
336 TSS capture respectively) (**Figure 2-II**). When the final velocity gradient of 20 s⁻¹ was increased
337 from one to five minutes, the fraction of flocs settling faster than 1.5 m³/m²/h increased (36% ±
338 4%) (**Figure 2-II**). This indicated that high shear forces followed by sufficiently a long low-
339 velocity gradient could help by (1) encouraging the formation of faster settling flocs by potentially
340 by rearranging floc structures, (2) promoting the formation of bigger flocs, and (3) improving
341 enmeshment of fines within the flocs. When a final velocity gradient of 90 s⁻¹ was applied for five
342 minutes, the TSS capture at 1.5 m³/m²/h was similar to the continuous shear experiment (11% ±
343 3% vs 10% ± 2% respectively). The capture was completely lost (0%) when 90 s⁻¹ was applied
344 for one minute at the end. This indicated that high shear forces applied for even a brief amount of
345 time can have detrimental effects on solids separation without adequate time under low shear
346 conditions to reverse the floc breakage.

347 **3.3. Continuous clarifier tests to understand effects shear and SOR**

348 While batch experiments are a good tool to fingerprint the impact of shear on the settling velocity
349 distribution, they fail to provide representative effluent suspended solids one might expect in a
350 full-scale system due to scale constraints. Additionally, batch settling experiments are not entirely
351 representative for continuous flow systems, given that no underflow exists for batch settling. For
352 this reason, the impact of high (250 s⁻¹) and low (19 s⁻¹) shear, SOR, and sludge loading rate
353 (SLR) on effluent suspended solids was tested in a pilot-scale, continuous, clarifier (**Figure 3-**
354 **III**). Two sludge types were tested. One originated from the full-scale step-feed reactor operating
355 at an average SRT of 1.5 ± 0.5 days, F/M ratio of 3.0 ± 0.8 kg COD/g VSS/d, and SOR of 1.4 ±
356 0.2 m³/m²/h. The other sludge was sampled from the contact-stabilization pilot, which was
357 subjected to an average SRT of 1.4 ± 0.5 days, F/M ratio of 11.2 ± 3.7 kg COD/g VSS/d, and
358 SOR of 1.1 ± 0.1 m³/m²/h. **Table 3** gives the EPS quality and quantity associated with the two
359 sludge types. CS had a significantly higher amount of EPS and was of better quality than SF. CS
360 also produced larger flocs within the clarifier as 25% of the CS flocs had a Feret diameter larger
361 than 3.4 mm, compared to 1.6 mm for SF flocs (**Figure S3**).

362 Under low shear conditions (19 s^{-1}), CS sludge achieved a significantly lower effluent suspended
363 solids ($38 \pm 1 \text{ mg TSS/L}$) than SF sludge ($69 \pm 4 \text{ mg TSS/L}$) at $0.6 \text{ m}^3/\text{m}^2/\text{h}$. Only when the
364 clarifier solids inlet concentration was increased to 869 mg TSS/L (i.e. increasing the amount of
365 collisions), was SF able to achieve a similar effluent quality ($38 \pm 4 \text{ mg TSS/L}$) (**Figure 3-III**).
366 When the SOR was increased to $1.5 \text{ m}^3/\text{m}^2/\text{h}$, the effluent suspended solids increased on average
367 with 9 and 42 mg TSS/L for SF and CS testing, respectively. This indicated that most CS flocs
368 settled between $0.6 - 1.5 \text{ m}^3/\text{m}^2/\text{h}$, which is the typical operational range of HRAS clarifiers,
369 while the sensitivity toward SOR changes was larger for CS. The former was confirmed by batch
370 settling experiment in **Figure 3-I/II**, where under bioflocculation promoting conditions (19 s^{-1}),
371 $26\% \pm 13 \%$ of SF settled between $0.6-1.5 \text{ m}^3/\text{m}^2/\text{h}$ compared to $50\% \pm 5\%$ for CS (**Figure 3-II**).
372 A similar trend could be observed without mixing energy (**Figure 3-I**). The increase was also in
373 line with what was observed in the pilot during continuous operation, as the resulting ESS fits the
374 curve well (**Figure 4**).

375 When sludge was subjected to harsh shear (250 s^{-1}) for 10 minutes prior to being introduced to
376 the clarifier, a significant increase in effluent suspended solids was observed for all scenarios
377 (**Figure 3-III**). At an SOR of $0.6 \text{ m}^3/\text{m}^2/\text{h}$, applying a velocity gradient of 250 s^{-1} induced a $10 \pm$
378 3 mg TSS/L increase in effluent suspended solids of regardless of sludge type or feed
379 concentration. This indicated desorption of fines rather than floc formation limitation. When the
380 SOR was increased to $1.5 \text{ m}^3/\text{m}^2/\text{h}$, the CS sludge experienced a significantly bigger impact of
381 shear compared to the SF system. Whereas SF increased by $20 \pm 7 \text{ mg TSS/L}$, the 250 s^{-1} velocity
382 gradient induced a $45 \pm 3 \text{ mg TSS/L}$ increase for CS at $1.5 \text{ m}^3/\text{m}^2/\text{h}$, indicating an increased
383 sensitivity to changes in SOR when high shear was applied. Shear management is thus imperative
384 when bioflocculation is managed in CS system.

385 **3.4. Impact of fines loading on effluent suspended solids**

386 At Blue Plains advanced wastewater treatment plant, the waste originating from pre-dewatering
387 (solids processing return, SPR) is sent back to the secondary reactors for treatment. This waste is
388 a combination of dissolved air flotation effluent and centrifuge reject liquid. The stream thus
389 contains everything that was not captured in these processes, thus inherently rich in fines. The
390 average TSS in the SPR stream within the timeframe of **Figure 5** was $885 \pm 401 \text{ mg TSS/L}$. From
391 January 16 until 21, the SPR flow to the SF reactor was on average $0.12 \pm 0.03 \text{ kg TSS}_{\text{SPR}}/\text{kg}$

392 MLSS/d, where after it was fully redirected to the parallel “West” reactor on January 21 (**Figure**
393 **5**). After a brief upset in the reactor due to wet weather, the effluent suspended solids decreased
394 significantly with an average of 10 mg TSS/L from 40 ± 5 to 30 ± 6 mg TSS/L ($p = 0.003$).

395 4. Discussion

396 4.1. Role of biomass and EPS on capturing fines

397 Fines were defined as suspended solids that settle slower than $0.6 \text{ m}^3/\text{m}^2/\text{h}$, and therefore will not
398 be separated in a clarifier unless enmeshed into a bioflocculated floc. Bioflocculation is mediated
399 though EPS (Sheng et al., 2010), which can be provided through the active biomass fraction in
400 the wastewater, microbial growth (Rahman et al., 2019), and supplemented by bioaugmentation
401 of BNR sludge (Van Winckel et al., 2019). In this study, CEPT removed a large amount of
402 settleable solids and active heterotrophic fraction, thus EPS could only be formed through growth
403 (CS + SF) or seeded with bioaugmentation (SF). Additionally, solids removal could only be
404 achieved with proper bioflocculation given the lack of fast settling solids fed from the influent.
405 The higher EPS concentration found in contact-stabilization are in line with previous studies,
406 where a higher EPS production was found when sludge was subjected to a feast-famine regime
407 (Meerburg et al., 2016a; Rahman et al., 2017). An increase in EPS amount and quality (PN/PS-
408 ratio) was correlated with an increase in capture of fines, as CS configuration had both higher
409 EPS quantity/quality and better capture of fines as indicated by the lower ESS obtained at 0.6
410 $\text{m}^3/\text{m}^2/\text{h}$ (**Figure 3**). This was also in agreement with previous work on a similar wastewater
411 composition (Van Winckel et al., 2019). However, Kinyua et al. (2017) did not find a similar
412 correlation for an A-stage HRAS configuration, presumably because of the nature of the influent
413 (raw sewage vs CEPT-effluent). As such, for systems operating on CEPT-effluent, fines were
414 best managed by promoting EPS formation through going from step-feed to plug-flow (F/M
415 increase) or by shifting to contact-stabilization (feast-famine). Whether the bioflocculation
416 differences between CS and SF can be attributed to the loosely-bound (LB) or tightly-bound (TB)
417 fractions of the EPS remains unclear. This EPS fractionation was not performed in this study, as
418 no agreed definition of what defines the LB and TB fractions exist and are moreover highly
419 dependent on the extraction method. Existing research has therefore conflicting evidence, where
420 some cite a negative correlation between bioflocculation and LB (Li and Yang, 2007), while other
421 mainly attribute bioflocculation to the TB fraction (Liu et al., 2010). Additionally, EPS is also
422 important for the capture of colloidal COD, which has the same trend as fines (Jimenez et al.,
423 2015).

424 Bioflocculation can also be improved by increasing the mixed liquor concentrations in the reactor,
425 essentially increasing the total number of collisions in the clarifier, negating the impact of poorer
426 collision efficiency. The effluent suspended solids observed for SF in **Figure 3** was achieved with
427 a TSS-limited clarifier. Increasing the concentration improved the effluent quality as more
428 collisions led to higher chance of fines enmeshing in the flocs. At fixed influent characteristics
429 and loading rate, increasing the mixed liquor in the reactor is synonymous to increasing the SRT,
430 which translates into sacrificing some carbon redirection to ensure carbon capture. The balance
431 between carbon redirection and capture will depend on influent characteristics and temperature
432 and is thus plant specific. Controlling on oxygen uptake rate, rather than SRT, takes these
433 conditions into account (Van Winckel et al., 2018). Additionally, the degree of bioflocculation
434 (collision efficiency) can be measured with the threshold of flocculation (TOF) parameter
435 (Mancell-Egala et al., 2017), which can be helpful in determining the bioflocculation impairment
436 is present without relying solely on ESS numbers. Furthermore, Ngo et al. 2021 determined that
437 a relationship exists between TOF and ESS which can be implemented in a process model, helping
438 future modelling efforts to optimize HRAS clarifiers.

439 **4.2. Role of SOR and shear on effluent suspended solids**

440 The SOR is a critical yet often overlooked design parameter for HRAS systems. The SOR applied
441 at the high-rate contact-stabilization pilot and full-scale step feed were in range of the typical
442 SOR applied in the A-stage reactors in the Netherlands (0.75 - 1.4 m³/m²/h) (De Graaff & Roest,
443 2012). An elevated SOR puts pressure on the flocs, requiring an overall faster settling velocity
444 distribution if one wants adequate effluent quality. SOR itself can only be lowered by increasing
445 the number of clarifiers, requiring large capital investments and the required land to do so.
446 Managing the settling velocity distribution of the sludge thus is the only way to manage the impact
447 of SOR on effluent quality.

448 The effect of shear on the settling velocity distribution was dependent on the velocity gradient
449 applied prior to introduction into the clarifier. At low shear, flocculation will be promoted thus
450 providing a more favorable and faster settling velocity distribution. At high shear, floc breakup
451 will be dominant, leading to an overall slower distribution. This was especially true when
452 bioflocculation was adequate, as inducing high shear on the CS sludge led to a stark shift in
453 settling velocity distribution, deteriorating the effluent suspended solids as a result. In essence,

454 shear cannot be easily separated from SOR because changes in settling distribution will lead to
455 different impacts of SOR on the effluent suspended solids. Maximizing carbon capture therefore
456 should include creating the most optimal settling velocity distribution possible through EPS-
457 mediated bioflocculation and maintain that distribution when the sludge is introduced into the
458 clarifier.

459 A common hypothesis postulates that applying a high SOR will over time will shift the settling
460 velocity distribution to the right and might eventually lead to granulation (Beun et al., 1999).
461 However, no evidence of selection of fast settling aggregates in HRAS systems due to elevated
462 SOR have been observed in this study. One hypothesis may be that HRAS' microbiome is too
463 fast growing for this selection to take place and the SOR is too low to be selective enough.
464 Significant differences in microbiome between a high-rate and low-rate activated sludge were
465 found in the Netherlands (Meerburg et al., 2016b). Physical selectors, like a screen of cyclone
466 using for deammonification, could artificially increase the selection pressure on the sludge
467 without jeopardizing effluent quality (Wett et al., 2015). There are indications that this hold true
468 for selective retention of phosphate accumulating bacteria (Ford et al., 2016). However, further
469 research will have to show the design and effectiveness of a physical selector for continuous
470 HRAS applications.

471 **4.3. Technology solutions to manage fines capture and optimize the settling velocity** 472 **distribution**

473 The capture of fines and the resulting final settling velocity distribution of the sludge can be
474 managed by smart clarifier inlet design which minimizes inlet shear with or without flocculation
475 zones to ensure full flocculation. Furthermore, sludge introduced to the clarifier can be fed
476 through the sludge blanket. Multiple technologies exist that actively try to mitigate effluent
477 suspended solids. While most are designed for conventional systems, they should be transferable
478 to HRAS-type of applications.

479 Computational fluid dynamics (CFD) is a tool which can help designing proper clarifier geometry
480 and pick the right inlet and baffle design (Samstag et al., 2016). When linked to population
481 balances, the impact of hydrodynamic shear on floc formation/breakup can be estimated (Nopens
482 et al., 2015). Hydraulic flows can also be assessed with acoustic doppler measurements to identify
483 high shear areas in-situ and validate potential changes (Kinnear & Deines, 2001). The inlet

484 preferably includes a flocculation zone, which provides ample low shear conditions prior to
485 entering the clarifier in combination with smart baffle design helps in retaining the maximum
486 settling velocity distribution, especially after higher shear conditions in the channel (**Figure 2-**
487 **III**). Special considerations should further be given to appropriate baffle design to fully dissipate
488 the kinetic energy. This will be especially true for high-rate activated sludge systems that deal
489 with higher flow rates. Double perforated baffles could help dissipate the energy in rectangular
490 tanks (Lee, 2017). Circular clarifiers could on the other hand benefit from an energy-dissipating
491 inlet design (Shaw et al., 2005).

492 Feeding through a sludge blanket filters the feed through a sludge bed, maximizing the number
493 of collisions that take place. This would mean that any floc breakage that occurred prior to clarifier
494 will be nullified as the sludge will very rapidly reflocculate within the blanket. This allows for
495 instantaneous capture of fines and disconnects the SOR from the sludge's (floculent) settling
496 velocity distribution. Multiple technologies are commercially available. The Hydrograv Adapt
497 technology utilizes an adaptable feed height so that it always feeds below sludge blanket (Benisch
498 et al., 2018).

499 The Hydrograv Adapt however relies on a sufficiently high blanket level present, which requires
500 longer residence times within the clarifier. Given that high-rate systems operate at very short SRT
501 and HRT, extending the residence time in the clarifiers may lead to increased total sludge age,
502 thus inaccurately estimating the SRT in the reactor. In addition, desorption may happen due to
503 increased anaerobic residence times. This issue can be mitigated by shifting to a AAA™
504 (Alternated Activated Adsorption) process. AAA is a retrofitted primary clarifier which is act as
505 primary settler and A-stage combined in one tank where the feed is introduced through the settled
506 sludge bed (Wett et al., 2020).

507 The main culprit of sludge bed feeding is the sensitivity to wet-weather flow. Sudden changes in
508 flow may lead to turbulent conditions which can upset the bed, causing elevated effluent
509 suspended solids or in extreme cases clarifier failure. The Hydrograv mitigates this issue by
510 having a dynamic feed height which, e.g. through CFD, could be calibrated to certain heights
511 given a specific sludge blanket height (Benisch et al., 2018). The clarifier was able to handle up
512 to 700 gal/ft²/d (~ 1.2 m³/m²/h) without sacrificing on effluent quality, which could make it
513 appropriate for high-rate applications. Ultimately, novel innovations in clarifier design will be

514 necessary to accommodate the shear-prone, slower settling velocity distribution created by HRAS
515 and ensure excellent year-round performance in terms of effluent quality.

516 **5. Conclusion**

517 Overall, this work clarified the impact of process configuration, SOR, and shear on effluent
518 suspended solids in high-rate activated sludge systems solely driven by bioflocculation. The
519 following can be concluded from this study:

- 520 • Managing the loading and capture of fines ($< 0.6 \text{ m}^3/\text{m}^2/\text{h}$) to high-rate activated sludge
521 systems can significantly improve (i.e. lower) effluent suspended solids levels. An estimated
522 10 mg TSS/L of the effluent suspended solids was attributed to fines in the plug-flow
523 configuration. A switch to contact-stabilization could potentially decrease the effluent
524 suspended solids up to 31 mg TSS/L. Clarifier development focusing on sludge blanket
525 filtration can further improve ESS under dry weather conditions.
- 526 • High-rate activated sludge systems with a good quantity and quality of extracellular polymeric
527 substances (like the contact-stabilization process) are efficient in capturing fines but create
528 flocs with a narrow settling velocity distribution with a low average velocity. This makes the
529 system sensitive to surface overflow rate changes, because $50\% \pm 5\%$ of the mass has a
530 settling velocity between $0.6\text{-}1.5 \text{ m}^3/\text{m}^2/\text{h}$.
- 531 • Allowing for orthokinetic flocculation at a low velocity gradient (20 s^{-1}) for at least 1 minute
532 before clarification can safeguard the optimal the settling velocity distribution independent
533 of tank shear conditions. This highlights the importance of feed well design and 3D
534 distribution profile of clarifiers.

535 **Acknowledgments**

536 This work was supported by the Water Environment and Research Foundation [grant number
537 U1R14] and the National Science Foundation GOALI [grant number 1512667].

538 **References**

- 539 Alloul, A., Ganigue, R., Spiller, M., Meerburg, F., Cagnetta, C., Rabaey, K., Vlaeminck, S.E.
540 2018. Capture-Ferment-Upgrade: A Three-Step Approach for the Valorization of Sewage
541 Organics as Commodities. *Environ Sci Technol*, **52**(12), 6729-6742.
- 542 APHA. 2005. *Standard methods for the examination of the water and wastewater*, Washington,
543 DC.
- 544 Bailey Jr, W.F., Murthy, S.N., Benson, L., Constantine, T., Daigger, G.T., Sadick, T.E.,
545 Katehis, D. 2008. Method for nitrogen removal and treatment of digester reject water in
546 wastewater using bioaugmentation.
- 547 Balemans, S., Vlaeminck, S.E., Torfs, E., Hartog, L., Zaharova, L., Rehman, U., Nopens, I.
548 2020. The Impact of Local Hydrodynamics on High-Rate Activated Sludge Flocculation in
549 Laboratory and Full-Scale Reactors. *Processes*, **8**(2).
- 550 Benisch, M., Neethling, J., Hammer, G., Armbruster, M. 2018. Stress Testing of a Secondary
551 Clarifier with an Adaptive Inlet Structure. *Proceedings of the Water Environment Federation*.
552 pp. 5133-5147.
- 553 Beun, J.J., Hendriks, A., Van Loosdrecht, M.C.M., Morgenroth, E., Wilderer, P.A., Heijnen, J.J.
554 1999. Aerobic granulation in a sequencing batch reactor. *Water Research*, **33**(10), 2283-2290.
- 555 Biggs, C.A., Lant, P.A. 2000. activated sludge flocculation: on-line determination of floc size
556 and the effect of shear. *Water Res*, **34**(9), 2542-2550.
- 557 Cagnetta, C., Saerens, B., Meerburg, F.A., Decru, S.O., Broeders, E., Menkveld, W.,
558 Vandekerckhove, T.G.L., De Vrieze, J., Vlaeminck, S.E., Verliefde, A.R.D., De Gusseme, B.,
559 Weemaes, M., Rabaey, K. 2019. High-rate activated sludge systems combined with dissolved
560 air flotation enable effective organics removal and recovery. *Bioresour Technol*, **291**, 121833.
- 561 Camp, T.R., Stein, P.G. 1943. Velocity gradients and internal work in fluid motion. *J. Boston*
562 *Soc. Civ. Eng.*, **30**, 219-230.
- 563 Coombs, J. 1922. Improvements in or connected with the treatment of sewage and other impure
564 liquids. *Brit. Patent* 187, 315.
- 565 De Graaff, M., Roest, K. 2012. Inventarisatie van AB-systemen - optimale procescondities in de
566 A-trap. KWR.
- 567 DuBois, M., Gilles, K.A., Hamilton, J.K., Rebers, P., Smith, F. 1956. Colorimetric method for
568 determination of sugars and related substances. *Anal. Chem.*, **28**, 350-356.

569 EPA. 2013. Report on the Performance of Secondary Treatment Technology. EPA. EPA-821-R-
570 13-001.

571 Ford, A., Rutherford, B., Wett, B., Bott, C. 2016. Implementing Hydrocyclones in Mainstream
572 Process for Enhancing Biological Phosphorus Removal and Increasing Settleability through
573 Aerobic Granulation. *Proceedings of the Water Environment Federation*, 2016(9), 2798-2811.

574 Furukawa, H., Kato, Y., Inoue, Y., Kato, T., Tada, Y., Hashimoto, S. 2012. Correlation of
575 power consumption for several kinds of mixing impellers. *International Journal of Chemical*
576 *Engineering*, 2012.

577 Godfrey, J., Obi, F.N., Reeve, R. 1989. Measuring drop size in continuous liquid-liquid mixers.
578 *Chemical engineering progress*, 85(12), 61-69.

579 Guellil, A., Thomas, F., Block, J.-C., Bersillon, J.-L. and Ginestet, P. 2001. Transfer of organic
580 matter between wastewater and activated sludge flocs. *Water Research* **35**(1), 143-150.

581 Jimenez, J., Miller, M., Bott, C., Murthy, S., De Clippeleir, H., Wett, B. 2015. High-rate
582 activated sludge system for carbon management--Evaluation of crucial process mechanisms and
583 design parameters. *Water Res*, 87, 476-82.

584 Kinnear, D.J., Deines, K. 2001. Acoustic Doppler Current Profiler Clarifier Velocity
585 Measurement. *Proceedings of the Water Environment Federation*, 2001(9), 500-515.

586 Kinyua, M.N., Elliott, M., Wett, B., Murthy, S., Chandran, K., Bott, C.B. 2017. The role of
587 extracellular polymeric substances on carbon capture in a high rate activated sludge A-stage
588 system. *Chemical Engineering Journal*, 322, 428-434.

589 Lee, B. 2017. Evaluation of Double Perforated Baffles Installed in Rectangular Secondary
590 Clarifiers. *Water*, 9(6).

591 Li, X.Y. and Yang, S.F. 2007. Influence of loosely bound extracellular polymeric substances
592 (EPS) on the flocculation, sedimentation and dewaterability of activated sludge. *Water Res*,
593 41(5), 1022-1030.

594 Li, Z.H., Kuba, T., Kusuda, T., Wang, X.C. 2008. A Comparative Study on Aerobic Granular
595 Sludge and Effluent Suspended Solids in a Sequence Batch Reactor. *Environmental*
596 *Engineering Science*, 25(4), 577-584.

597 Liu, X.-M., Sheng, G.-P., Luo, H.-W., Zhang, F., Yuan, S.-J., Xu, J., Zeng, R.J., Wu, J.-G. and
598 Yu, H.-Q. 2010. Contribution of extracellular polymeric substances (EPS) to the sludge
599 aggregation. *Environmental science & technology*, 44(11), 4355-4360.

600 Lowry, O.H., Rosebrough, N.J., Farr, A.L., Randall, R.J. 1951. Protein measurement with the
601 Folin phenol reagent. *J Biol Chem*, **193**(1), 265-75.

602 Mamais, D., Jenkins, D., Pitt, P. 1993. A Rapid Physical-Chemical Method For The
603 Determination Of Readily Biodegradable Soluble COD In Municipal Wastewater. *Water Res*,
604 **27**(1), 195-197.

605 Mancell-Egala, W., De Clippeleir, H., Su, C., Takacs, I., Novak, J.T., Murthy, S.N. 2017. Novel
606 Stokesian Metrics that Quantify Collision Efficiency, Floc Strength, and Discrete Settling
607 Behavior. *Water Environ Res*, **89**(7), 586-597.

608 Mancell-Egala, W., Kinnear, D.J., Jones, K.L., De Clippeleir, H., Takacs, I., Murthy, S.N. 2016.
609 Limit of stokesian settling concentration characterizes sludge settling velocity. *Water Res*, **90**,
610 100-110.

611 Meerburg, F.A., Boon, N., Van Winckel, T., Pauwels, K.T., Vlaeminck, S.E. 2016a. Live Fast,
612 Die Young: Optimizing Retention Times in High-Rate Contact Stabilization for Maximal
613 Recovery of Organics from Wastewater. *Environ Sci Technol*, **50**(17), 9781-90.

614 Meerburg, F.A., Boon, N., Van Winckel, T., Vercamer, J.A.R., Nopens, I., Vlaeminck, S.E.
615 2015. Toward energy-neutral wastewater treatment: a high-rate contact stabilization process to
616 maximally recover sewage organics. *Bioresour Technol*, **179**, 373-381.

617 Meerburg, F.A., Vlaeminck, S.E., Roume, H., Seuntjens, D., Pieper, D.H., Jauregui, R.,
618 Vilchez-Vargas, R., Boon, N. 2016b. High-rate activated sludge communities have a distinctly
619 different structure compared to low-rate sludge communities, and are less sensitive towards
620 environmental and operational variables. *Water Res*, **100**, 137-145.

621 Metcalf, Eddy. 2003. *Wastewater Engineering: Treatment and Reuse*. McGraw-Hill Education.

622 Ngo, K.N., Van Winckel, T., Massoudieh, A., Wett, B., Al-Omari, A., Murthy, S., Takács, I.
623 and De Clippeleir, H., 2021. Towards more predictive clarification models via experimental
624 determination of flocculent settling coefficient value. *Water Research*, **190**, p.116294.

625 Murthy, S.N. (1998) Bioflocculation: implications for activated sludge properties and
626 wastewater treatment, Virginia Polytechnic Institute and State University.

627 Nopens, I., Torfs, E., Ducoste, J., Vanrolleghem, P.A., Gernaey, K.V. 2015. Population balance
628 models: a useful complementary modelling framework for future WWTP modelling. *Water Sci*
629 *Technol*, **71**(2), 159-67.

630 Rahman, A., De Clippeleir, H., Thomas, W., Jimenez, J.A., Wett, B., Al-Omari, A., Murthy, S.,
631 Riffat, R., Bott, C. 2019. A-stage and high-rate contact-stabilization performance comparison
632 for carbon and nutrient redirection from high-strength municipal wastewater. *Chemical*
633 *Engineering Journal*, **357**, 737-749.

634 Rahman, A., Meerburg, F.A., Ravadagundhi, S., Wett, B., Jimenez, J., Bott, C., Al-Omari, A.,
635 Riffat, R., Murthy, S., De Clippeleir, H. 2016. Bioflocculation management through high-rate
636 contact-stabilization: A promising technology to recover organic carbon from low-strength
637 wastewater. *Water Res*, **104**, 485-496.

638 Rahman, A., Mosquera, M., Thomas, W., Jimenez, J.A., Bott, C., Wett, B., Al-Omari, A.,
639 Murthy, S., Riffat, R., De Clippeleir, H. 2017. Impact of aerobic famine and feast condition on
640 extracellular polymeric substance production in high-rate contact stabilization systems.
641 *Chemical Engineering Journal*, **328**, 74-86.

642 Rahman, A., Yapuwa, H., Baserba, M.G., Rosso, D., Jimenez, J.A., Bott, C., Al-Omari, A.,
643 Murthy, S., Riffat, R. and De Clippeleir, H. 2017. Methods for quantification of biosorption in
644 high-rate activated sludge systems. *Biochemical Engineering Journal* **128**, 33-44.

645 Rinas, M., Tränckner, J., Koegst, T. 2018. Sedimentation of Raw Sewage: Investigations For a
646 Pumping Station in Northern Germany under Energy-Efficient Pump Control. *Water*, **11**(1).

647 Rocktäschel, T., Klarmann, C., Ochoa, J., Boisson, P., Sørensen, K., Horn, H. 2015. Influence
648 of the granulation grade on the concentration of suspended solids in the effluent of a pilot scale
649 sequencing batch reactor operated with aerobic granular sludge. *Separation and Purification*
650 *Technology*, **142**, 234-241.

651 Samstag, R.W., Ducoste, J.J., Griborio, A., Nopens, I., Batstone, D.J., Wicks, J.D., Saunders, S.,
652 Wicklein, E.A., Kenny, G., Laurent, J. 2016. CFD for wastewater treatment: an overview.
653 *Water Sci Technol*, **74**(3), 549-63.

654 Shaw, A., McGuffie, S., Wallis-Lage, C., Barnard, J. 2005. Optimizing Energy Dissipating Inlet
655 (Edi) Design in Clarifiers Using an Innovative Cfd Tool. *Proceedings of the Water Environment*
656 *Federation*, **2005**(6), 8719-8736.

657 Sheng, G.P., Yu, H.Q., Li, X.Y. 2010. Extracellular polymeric substances (EPS) of microbial
658 aggregates in biological wastewater treatment systems: a review. *Biotechnol Adv*, **28**(6), 882-94.

659 Sturm, B., Faraj, R., Amante, T., Kambhampati, S., Warren, J. 2016. Impact of Substrate Profile
660 on BNR Performance in Aerobic Granular Sludge Pilots at the Lawrence, KS WWTP.
661 *Proceedings of the Water Environment Federation*, **2016**(9), 5470-5478.

662 Ullrich, A. and Smith, M.W. 1951. The biosorption process of sewage and waste treatment.
663 *Sewage and Industrial Wastes*, 1248-1253.

664 Urbain, V., Block, J. and Manem, J. 1993. Bioflocculation in activated sludge: an analytic
665 approach. *Water research* **27**(5), 829-838.

666 Van Winckel, T., Liu, X., Vlaeminck, S.E., Takacs, I., Al-Omari, A., Sturm, B., Kjellerup,
667 B.V., Murthy, S.N., De Clippeleir, H. 2019. Overcoming floc formation limitations in high-rate
668 activated sludge systems. *Chemosphere*, **215**, 342-352.

669 Van Winckel, T., Olagunju, O., Sturm, B., Vlaeminck, S.E., Bott, C., Wett, B., Al-Omari, A.,
670 Murthy, S., De Clippeleir, H. 2018. Oxygen uptake rate control in high-rate contact stabilization
671 for effective carbon management. in: *IWA Nutrient Removal and Recovery Conference*.
672 Brisbane, Australia.

673 Wahlberg, E.J., Keinath, T.M., Parker, D.S. 1994. Influence of Activated Sludge Flocculation
674 Time on Secondary Clarification. *Water Environ. Res.*, **66**(6), 779-786.

675 WEF. 2005. *Clarifier Design: WEF Manual of Practice No. FD-8*. McGraw-Hill Professional.

676 Wett, B., Aichinger, P., Hell, M., Andersen, M., Wellym, L., Fukuzaki, Y., Cao, Y.S., Tao, G.,
677 Jimenez, J., Takacs, I., Bott, C., Murthy, S. 2020. Operational and structural A-stage
678 improvements for high-rate carbon removal. *Water Environ Res*, **92**(11), 1983-1989.

679 Wett, B., Podmirseg, S.M., Gomez-Brandon, M., Hell, M., Nyhuis, G., Bott, C., Murthy, S.
680 2015. Expanding DEMON Sidestream Deammonification Technology Towards Mainstream
681 Application. *Water Environ Res*, **87**(12), 2084-9.

682 **Tables**

683 **Table 1.** Influent and effluent characteristics of the contact stabilization pilot reactor runs. All average (and standard deviations) were calculated based on $n > 14$,
 684 except total Kjeldal N which was calculated based on $n > 3$.

	Influent			Effluent			
	<i>Scenario A</i>	<i>Scenario B</i>	<i>Scenario C</i>	<i>Scenario A</i>	<i>Scenario B</i>	<i>Scenario C</i>	
Total COD	218 ± 61	237 ± 39	232 ± 18	149 ± 39	141 ± 23	143 ± 27	mg COD/L
Particulate COD	98 ± 31	108 ± 36	112 ± 28	83 ± 23	63 ± 23	58 ± 27	mg COD/L
Colloidal COD	50 ± 17	85 ± 113	46 ± 21	13 ± 14	21 ± 23	24 ± 13	mg COD/L
Soluble COD	85 ± 17	72 ± 12	74 ± 17	57 ± 19	57 ± 7	58 ± 11	mg COD/L
Total Kjeldal N	41 ± 5	41 ± 8	68 ± 14	43 ± 10	42 ± 4	58 ± 3	mg N/L
Ammonia N	35 ± 3	34 ± 6	37 ± 4	34 ± 2	34 ± 5	36 ± 4	mg N/L
Total Phosphorus	2.4 ± 0.6	2.3 ± 0.5	2.7 ± 0.6	2.1 ± 0.8	1.6 ± 0.4	1.9 ± 0.7	mg P/L
Ortho-Phosphorus	1.2 ± 0.4	0.7 ± 0.4	1.1 ± 0.3	0.5 ± 0.3	0.2 ± 0.2	0.9 ± 0.3	mg P/L
Effluent suspended solid	57 ± 9	64 ± 19	61 ± 13	62 ± 19	49 ± 11	40 ± 15	mg TSS/L

685

686

687 **Table 2.** Process, clarifier parameters and extracellular polymeric substances (EPS) characteristics from the three
 688 scenarios operated on the contact-stabilization pilot reactor. The average of the process and clarifier parameters were
 689 calculated based on $n > 14$. EPS was calculated based on $n > 4$. PN = protein, PS = polysaccharide.

	<i>Scenario A</i>	<i>Scenario B</i>	<i>Scenario C</i>	
Process parameters				
Solids retention time	0.9 ± 0.5	1.0 ± 0.5	0.4 ± 0.3	d
Temperature	14.8 ± 2.3	15.1 ± 1.0	19.3 ± 1.5	°C
Dissolved oxygen	0.8 ± 0.8	0.0 ± 0.1	0.0 ± 0.1	mg O ₂ /L
Coarse bubble duration	7 ± 0	1 ± 0	1 ± 0	s
Coarse bubble frequency	4 ± 0	4 ± 0	4 ± 0	min ⁻¹
Coarse bubble air flow rate	4 ± 0	4 ± 0	4 ± 0	m ³ /h
Organic loading rate	5.5 ± 0.4	5.4 ± 0.8	5.0 ± 0.3	kg COD/m ³ /d
F/M rate (total COD)	26 ± 17	17 ± 3	30 ± 9	kg COD/kg VSS/d
F/M rate (soluble COD)	9.0 ± 5.6	5.1 ± 1.1	9.4 ± 3.7	kg COD _{ff} /kg VSS/d
Clarifier Parameters				
Surface overflow rate	1.0 ± 0.0	0.9 ± 0.1	0.6 ± 0.2	m ³ /m ² /h
Solids loading rate	9.2 ± 4.8	9.3 ± 2.7	2.9 ± 1.2	kg TSS/m ² /d
Extracellular polymeric substances (EPS)				
Total EPS	286 ± 42	233 ± 79	241 ± 67	mg COD/g VSS
Total EPS protein	65 ± 21	32 ± 3	34 ± 20	mg BSA/g VSS
Total EPS polysaccharide	36 ± 14	21 ± 6	25 ± 6	mg glucose/g VSS
Total EPS PN/PS ratio	1.8 ± 0.2	2 ± 0	1.4 ± 0.5	mg BSA/mg glucose

690

691

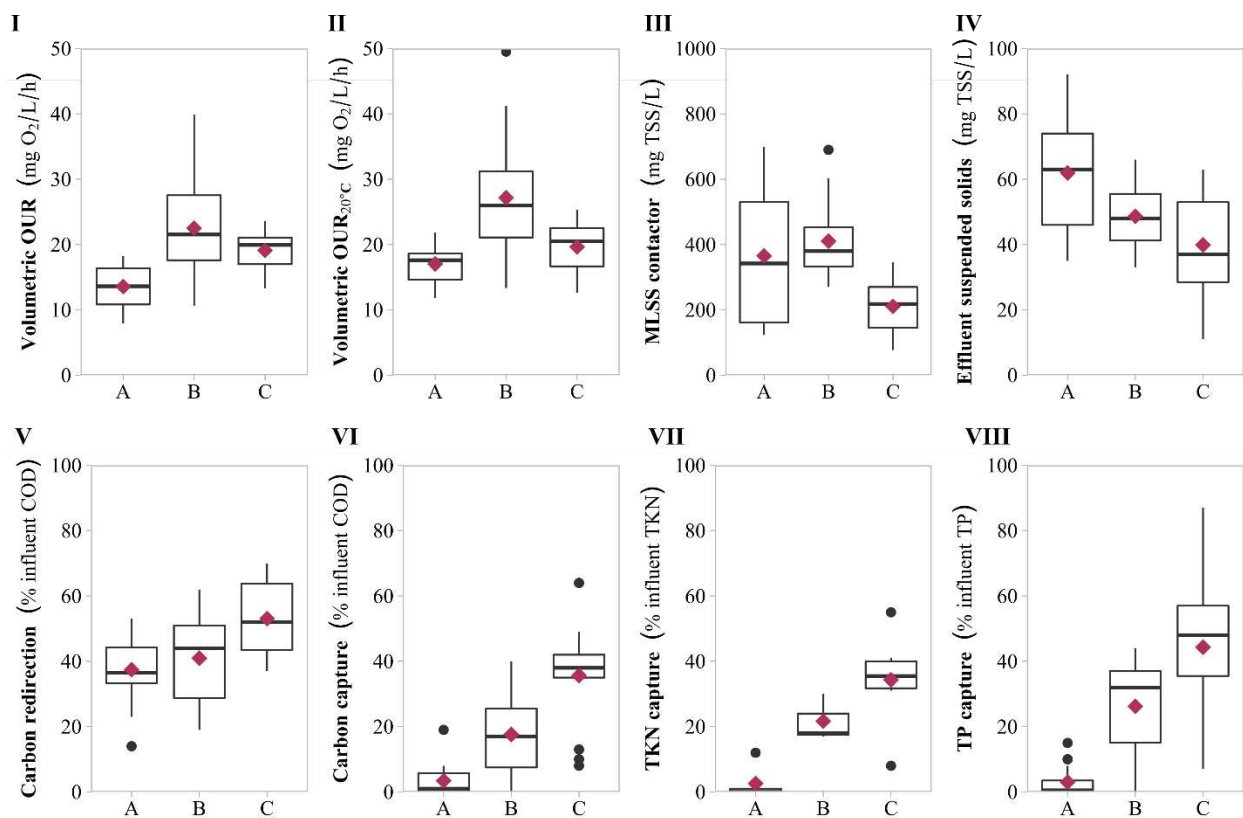
692

693 **Table 3.** Characteristics of the extracellular polymeric substances (EPS) of the full-scale step-feed and pilot-scale
 694 contact-stabilization reactor at the time of the clarifier experiments (n = 3, PN = protein, PS = polysaccharide).

Parameter	Contact-stabilization reactor			Step-feed reactor			Unit
Total EPS	235	±	22	177	±	11	mg COD/g VSS
Total EPS protein	66	±	3	42	±	21	mg BSA/g VSS
Total EPS polysaccharide	28	±	3	23	±	11	mg glucose/g VSS
Total EPS PN/PS ratio	2.4	±	0.3	1.8	±	0.3	mg BSA/mg glucose

695

696 **Figures**

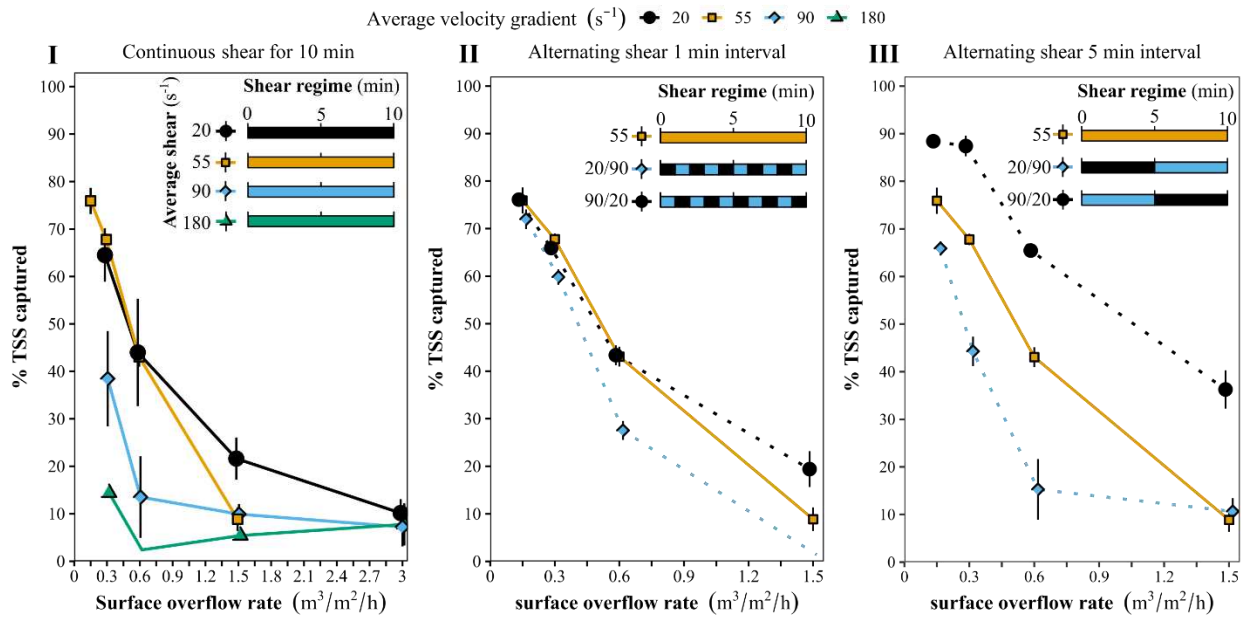


697

698 **Figure 1.** High-rate contact-stabilization pilot: boxplots of key biological and performance parameters of the three
 699 scenarios A, B and C (diamonds representing the average) The purple triangles indicate the data's average. **(I)**
 700 Volumetric OUR measured in the contactor. **(II)** Volumetric OUR in contactor corrected for temperature using the
 701 standard Arrhenius coefficient (1.04). **(III)** Mixed liquor concentration in the contactor. **(IV)** Effluent suspended
 702 solids. **(V)** Observed carbon redirection based on COD mass balancing. **(VI)** Percentage influent COD captured in the
 703 waste activated sludge. **(VII/VIII)** Percentage of TKN/TP capture.

704

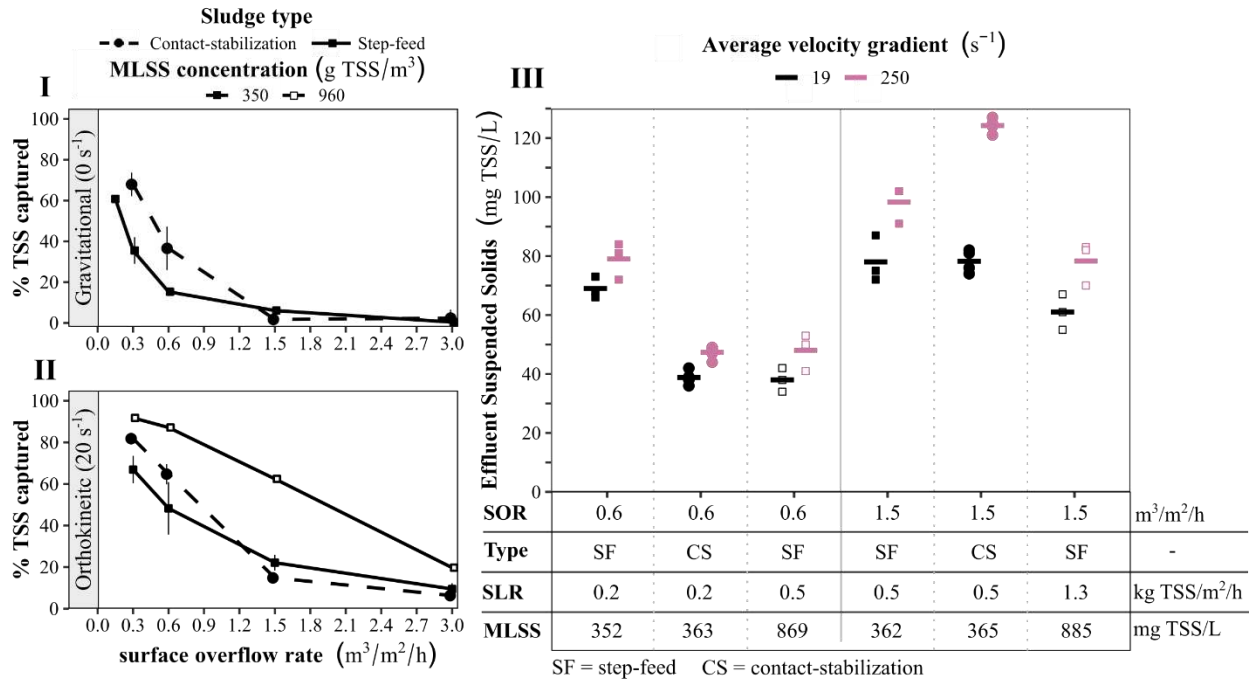
705



706

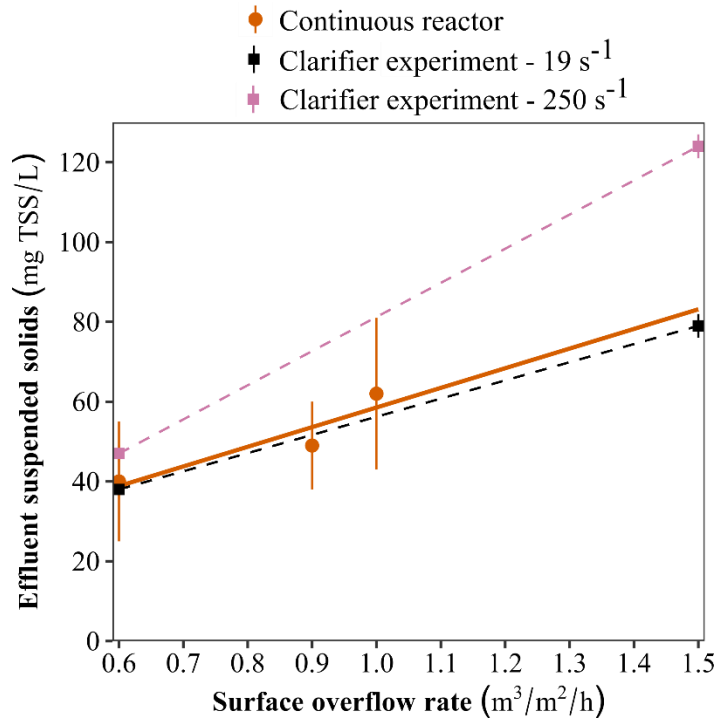
707 **Figure 2.** Effect of surface overflow rate on TSS capture in batch clarifier at different shear regimes. Sludge obtained
708 from full-scale plug-flow reactor. **(I)** continuous shear for 10 minutes, **(II)** shear interval where the velocity gradient
709 was alternating between $20 s^{-1}$ and $90 s^{-1}$ every minute for 10 minutes, and **(III)** shear interval with alternating velocity
710 gradients every 5 minutes for 10 minutes. The $55 s^{-1}$ line from panel A was repeated in panel B and C because its total
711 energy ($G \times t$) was equal to the alternating shear regimes.

712



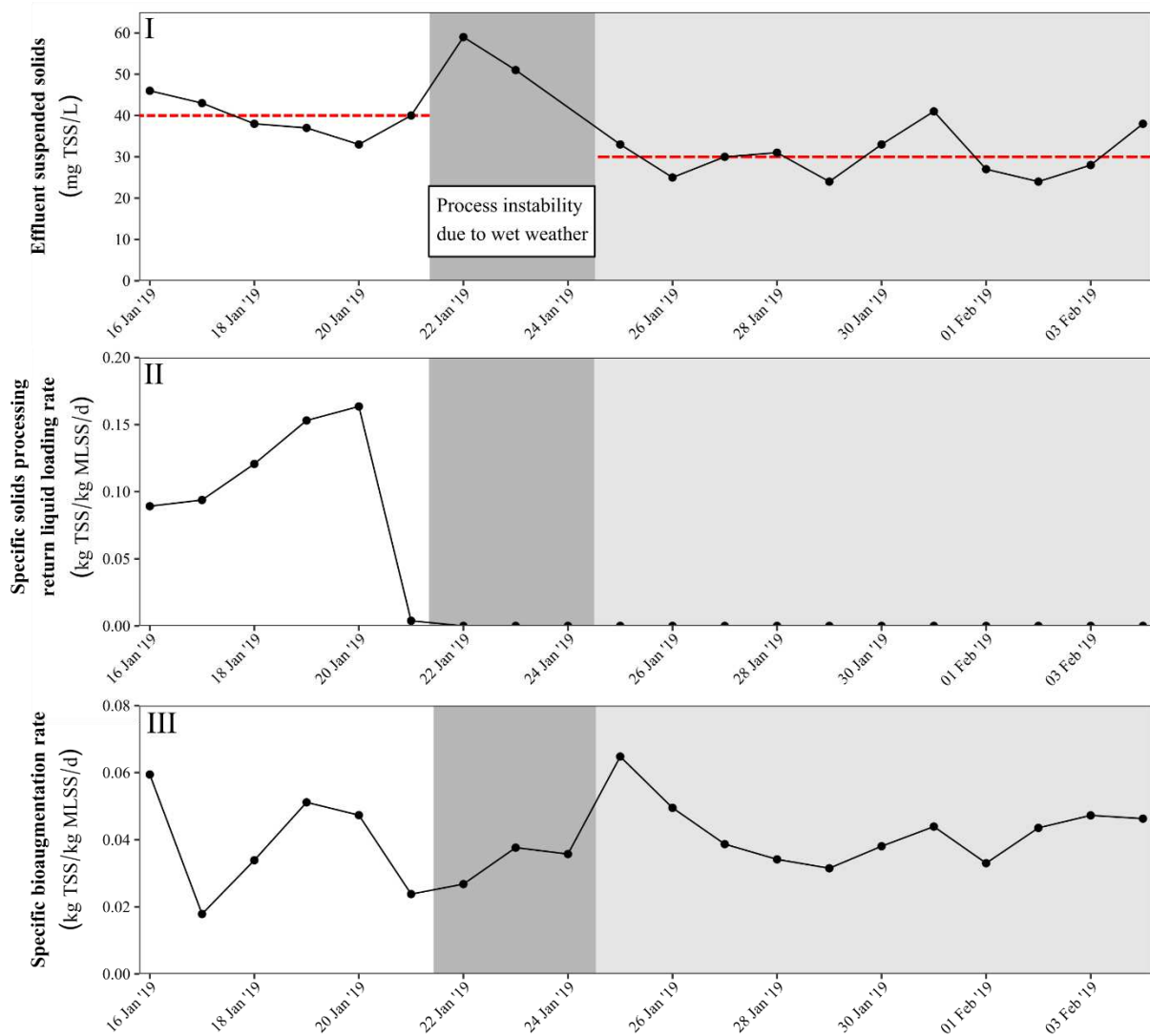
713

714 **Figure 3.** Continuous clarifier experiment with corresponding batch settling tests. **(I/II)** TSS capture obtained in batch
 715 settling tests at time of the continuous clarifier experiment in function of surface overflow rate in a gravitational (0 s⁻¹)
 716 ¹) **(I)** and orthokinetic (20 s⁻¹) **(II)** environment tested at 350 and 960 mg TSS/L. **(III)** Pilot-scale continuous clarifier
 717 experiment where the effluent suspended solids was investigated at 2 different surface overflow rates (0.6 and 1.5
 718 m³/m²/h) and velocity gradients (19 s⁻¹ vs 250 s⁻¹).



719

720 **Figure 4.** Effluent suspended solids obtained from the controlled clarifier experiment (squares) and continuous
 721 reactors (orange dots) of the contact stabilization reactor. The orange line denotes the linear regression trendline of
 722 the three points obtained from the continuous reactor. Dashed lines are for clarity only and not indicative of trends
 723 between the two datapoints.



724

725 **Figure 5.** Full-scale step-feed (SF) high-rate activated sludge reactor: Impact of colloid loading and bioaugmentation
 726 rate on the profiles of effluent suspended solids during a three-week period (**I**). The profiles are split up in a first period
 727 where the reactor received solids processing return liquid (levels in panel **II**; white background), with on average 40
 728 ± 5 mg TSS/L in the effluent. In the last period, the SF reactor did not receive return liquid, and following wet weather-
 729 related instability, the average ESS level was 30 ± 5 mg TSS/L (light gray background). The bioaugmentation rates
 730 are shown in (**III**).